UGP Report-
Laser Induced deformation and breakup of acuostically levitated Droplet

Presented By-Anil Yadav(210137)
Department of Aerospace Engineering, IIT Kanpur

Project Supervisor-Dr.D Chaitanya Rao

April 16, 2025

Abstract

Understanding laser-induced deformation and fragmentation of single droplet is crucial for various applications. Laser-induced breakup is explored for applications like surface cleaning, nano-lithography, microelectronics, and medical procedures.It can also be used in combustion engines to study fuel atomization and its impact on combustion efficiency and emissions. In this study, we investigate the response of acoustically levitated decane, ethanol, and xylene droplets when exposed to a continuous-wave CO_2 laser. The laser energy was varied at 20%, 40%, and 80% of the 10 W maximum capacity to induce deformation and breakup. A high-speed camera, synchronized with a dedicated light source, was used to capture the transient events. Distinct deformation modes were observed depending on the fluid properties and laser power. Ethanol showed rapid surface deformation and early breakup, while xylene and decane exhibited delayed fragmentation and larger-scale shape oscillations. The results offer insights into thermally driven, laser-induced droplet dynamics under acoustic levitation

1 Introduction

Droplet deformation and breakup are phenomena of critical importance in a range of engineering applications such as fuel atomization in combustion systems, pharmaceutical sprays, inkjet printing, and thermal control systems. While the fragmentation of droplets through mechanical or impulsive forces has been widely studied, the breakup behavior driven by localized thermal input—particularly using continuous-wave (CW) lasers—remains comparatively less explored.

In this work, we investigate the breakup mechanisms of acoustically levitated liquid droplets subjected to a focused infrared continuous-wave CO_2 laser. The study is carried out on three different single-component liquids—decane, ethanol, and xylene—to understand the effect of varying thermophysical properties such as boiling point, surface tension, viscosity, and optical absorption. By tuning the laser power to 20%, 40%, and 80% of its maximum output (10 W), we examine how the gradual energy absorption influences droplet deformation, oscillation, and eventual breakup.

The use of acoustic levitation provides a contact-free environment, enabling the study of undisturbed droplet dynamics in the presence of localized heating. A synchronized high-speed imaging system is used to record the droplet response with high temporal resolution. The continuous laser exposure in our study introduces internal pressure buildup, and surface instabilities that evolve over time, leading to shape oscillations and breakup mediated by vaporization,.

Our physical investigation focuses on identifying the conditions under which a droplet transitions from stable deformation to complete disintegration.The balance between internal pressure rise due to heating and the restoring force from surface tension is hypothesized to govern the onset of instability. Furthermore, the influence of thermal gradients on fluid motion within the droplet plays a crucial role in the evolution of surface disturbances that eventually cause rupture or disintegration.

Although prior studies have addressed laser-induced droplet breakup using ultrafast or nanosecond pulses primarily in dynamic environments, detailed investigations on breakup modes under steady-state thermal input, especially for acoustically levitated droplets, are limited. The present study aims to fill this gap by providing experimental insights into the breakup dynamics and mechanisms under continuous-wave laser irradiation. Our goal is to develop a better understanding of the interplay between laser power, material

properties, and breakup behavior, and to identify the critical physical parameters that dictate the transition from deformation to fragmentation.

2 Details of the Experimental Setup and Investigated Liquids

2.1 Laser Setup

Figure 1 illustrates the experimental setup consisting of a 10W CO_2 laser, an acoustic levitator, and a high-speed imaging system. A continuous-wave CO_2 laser (wavelength: 10,600 nm) with a maximum power output of 10 W was used to initiate droplet fragmentation. The laser beam, having an initial diameter of 3.5 mm, was expanded using a 5× beam expander and subsequently focused using a ZnSe lens of focal length 50.8 mm. The spot size at the focus was estimated to be approximately 50 μm, determined using a laser burn paper—burn marks became visible at maximum intensity when the focal point was reached. This spot size was significantly smaller than the droplet diameter, ensuring localized interaction during the laser-induced breakup.

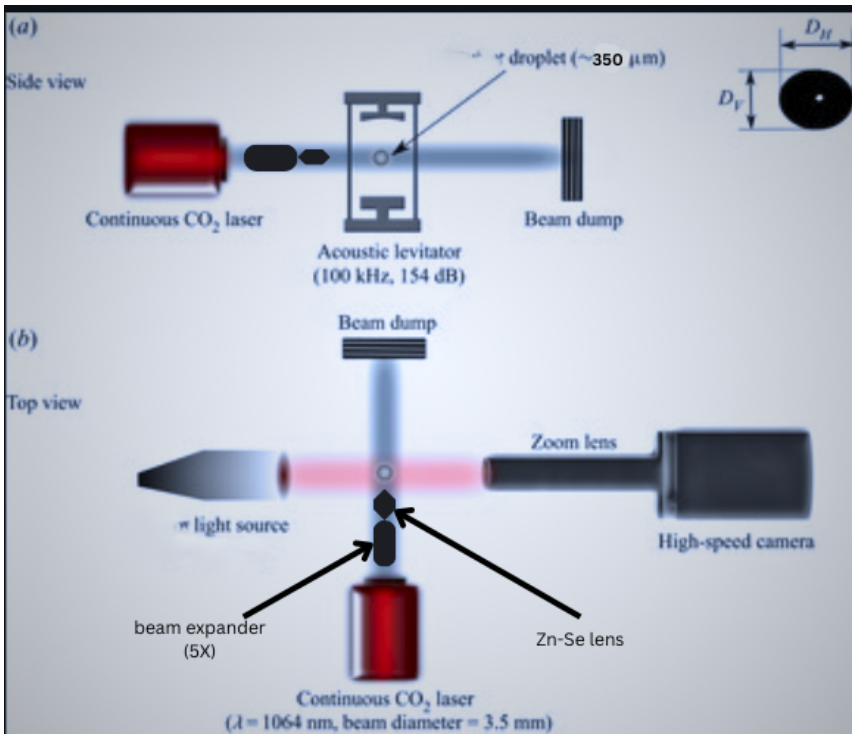

Figure 1: Schematic of the experimental setup used for CO_2 laser-induced fragmentation.

2.2 Laser Spot Size Calculation

The focused spot size (w_0) can be calculated using the Gaussian beam optics formula:

$$w_0 = \frac{4\lambda f}{\pi D}$$

Where:

- λ = Laser wavelength (10,600 nm)
- f = Focal length of the ZnSe lens (50.8 mm)
- D = Expanded beam diameter at the lens

The beam expander magnifies the initial laser beam diameter by 5×:

$$D_{\text{expanded}} = 3.5\,\text{mm} \times 5 = 17.5\,\text{mm} = 0.0175\,\text{m}$$

$$w_0 = \frac{4 \times (10.6 \times 10^{-6}\,\text{m}) \times (50.8 \times 10^{-3}\,\text{m})}{\pi \times 0.0175\,\text{m}}$$

$$w_0 = \frac{2.143 \times 10^{-6}\,\text{m}^2}{0.055\,\text{m}} = 39.11\,\mu\text{m}$$

Actual Spot Size with Beam Quality Factor $M^2 = 1.2$

For a non-ideal beam:

$$w_0^{\text{actual}} = \frac{4M^2\lambda f}{\pi D} = \frac{4 \times 1.2 \times (10.6 \times 10^{-6}) \times (50.8 \times 10^{-3})}{\pi \times 0.0175}$$

$$w_0^{\text{actual}} = \frac{2.5812 \times 10^{-6}}{0.055} = 46.93\,\mu\text{m}$$

2.3 Levitation and Droplet Generation

In this experiment, a commercial ultrasonic levitator (Tech5 AG) was used to levitate liquid droplets for laser-induced breakup studies. The device operates at a frequency of 100 kHz, producing a standing wave in ambient air that can trap small droplets at the antinodes.

Working Principle: Ultrasonic levitation relies on the generation of standing sound waves between an ultrasonic transducer and a reflector. When the spacing between them is a multiple of half the wavelength, a standing wave is formed with alternating pressure nodes and antinodes. Small samples with diameters less than half the wavelength can be trapped at these nodes due to acoustic radiation pressure and radial Bernoulli forces.

Specifications:

- Operating Frequency: 100 kHz
- Wavelength in air: ∼5.9 mm
- Operating Temperature: 0°C to +70°C

Droplet Size Used: In this study, a droplet size of approximately 350 µm was used, which is well within the levitator's optimal range for 100 kHz operation. This small size ensures stable levitation and minimal shape deformation during laser exposure.

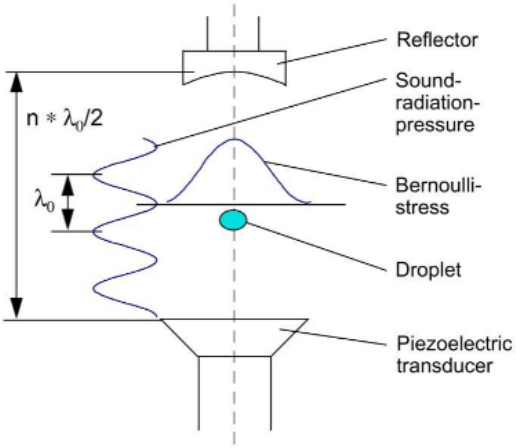

(a) schematic setup of lavitator and pressure distribution

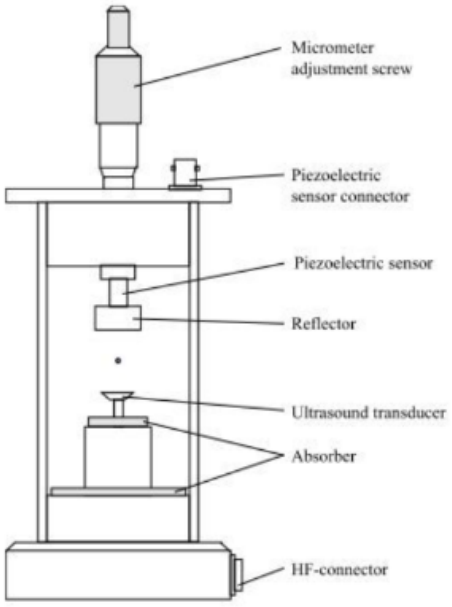

(b) schematic diagram of ultrasonic lavitator

2.4 Imaging System and Calibration

The fragmentation dynamics of the levitated droplets were captured using a high-speed camera (NOVA S6, Photron) operating at 50,000 frames per second. The camera had a resolution of 384 × 256 pixels. Illumination was provided through a light source with a diffuser setup to produce sharp images of the droplet and its breakup stages.

Calibration: To calibrate the imaging system, a needle of known diameter was placed at the exact position where the droplet levitation and breakup occurred. An image of the needle was captured, and the number of pixels spanning its diameter was measured. From this, the pixel-to-distance conversion factor was calculated as 0.013095 mm/px. This calibration was used in all spatial measurements and droplet size analysis during post-processing.

Synchronization: The camera was operated using the photron camera software, which was interfaced with the laser and light source systems. Once the camera setup was ready to capture, triggering the camera initiated the laser and lightsource simultaneously. This ensured synchronized image capture of the droplet's breakup dynamics right from the laser interaction.

2.5 Properties of the Investigated Liquids

Three different liquids were investigated in the present study: ethanol, decane, and xylene. These liquids were selected due to their varying thermo-physical properties such as surface tension, viscosity, and volatility, all of which influence the breakup dynamics under laser irradiation. The standard physical properties of these liquids at room temperature (293 K) are summarized in Table 1.

Table 1: Physical properties of investigated fuels at 293 K (standard values).

Property	**Ethanol**	***n*-Decane**	**Xylene**
Density (kg/m^3)	789	730	861
Viscosity (mPa·s)	1.2	0.92	0.65
Surface tension (N/m)	0.022	0.0258	0.028
Boiling point (K)	351	447	412
Specific heat (kJ/kg·K)	2.44	2.22	1.72

3 Results and Discussion

3.1 Temporal Evolution of Xylene Droplet Breakup at Different Energies

Figures 3, 4, and 5 show the fragmentation of xylene droplets at 20%, 40%, and 80% laser power respectively.

The laser-induced breakup of xylene droplets was analyzed at three different energy levels: 20%, 40%, and 80% of maximum laser power. The evolution of the breakup process was captured at high temporal resolution, revealing distinct breakup mechanisms corresponding to each power setting.

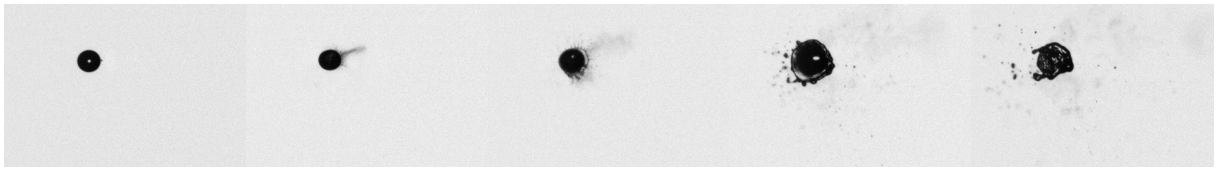

Figure 3: Breakup of xylene droplet at 20% laser power.

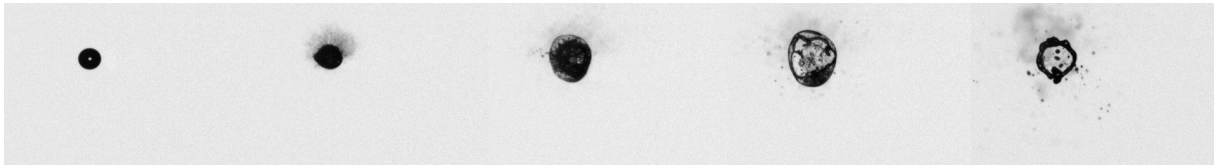

Figure 4: Breakup of xylene droplet at 40% laser power.

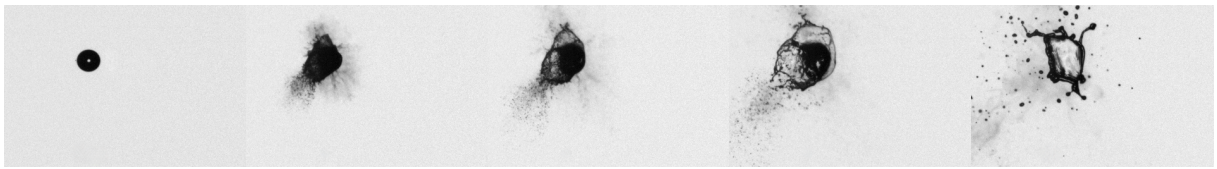

Figure 5: Breakup of xylene droplet at 80% laser power.

At 20% power, the breakup was relatively mild. The initial rupture occurred at approximately $t = 30.4$ ms, where a tiny burst was observed at the droplet surface. This was followed by the formation of a thin film, which gradually evolved into ligaments. These ligaments underwent secondary breakup, ultimately forming smaller droplets. The overall deformation was less intensive, with breakup proceeding in a delayed and sequential manner.

At 40% power, the first sign of rupture appeared earlier, around $t = 24.4$ ms. The initial burst was slightly more pronounced than that at 20%. Following this, the droplet began to flatten and expand outward, forming a liquid sheet. This sheet grew thicker along the edges due to accumulation of mass, which then destabilized and led to ligament formation and droplet disintegration. The breakup process was faster and more intense compared to the 20% case.

At 80% power, the breakup occurred very rapidly and violently. The first rupture was recorded at $t = 16$ ms, characterized by an abrupt burst. Immediately after, a bag-like structure formed around the droplet, likely due to rapid expansion from internal pressure. This structure quickly lost stability, resulting in complete disintegration of the droplet into smaller fragments. The entire process was highly energetic and occurred in a short span of time.

These observations clearly indicate that the breakup intensity and timing are strongly dependent on the input laser energy. Higher power levels induce more violent and rapid breakup due to increased localized energy deposition and internal pressure build-up within the droplet.

3.2 Comparative Study of different fuels at 80% Laser Power

The first breakup behavior of ethanol, n-decane, and xylene was investigated at 80% of the laser's maximum power. The laser-induced deformation and breakup showed distinct characteristics for each liquid, largely influenced by their physical and thermophysical properties such as viscosity, volatility, surface tension, and absorption of the infrared CO_2 laser radiation.

Ethanol exhibited its first breakup at $t = 9.28$ ms. The breakup was characterized by a gentle ejection of mass in the form of a fine mist or minute droplets, resembling a vapor-like outflow. This behavior can be attributed to ethanol's relatively low boiling point (78.37°C) compared to the other two liquids.Ethanol also exhibits lower infrared absorption in the 10.6 μm wavelength range of the CO_2 laser, resulting in a more surface-limited energy deposition. These properties favor rapid vaporization and surface evaporation when exposed to intense thermal energy. This likely leads to localized heating and phase change at the droplet surface, without substantial internal pressure buildup, hence producing a soft mist-like breakup.

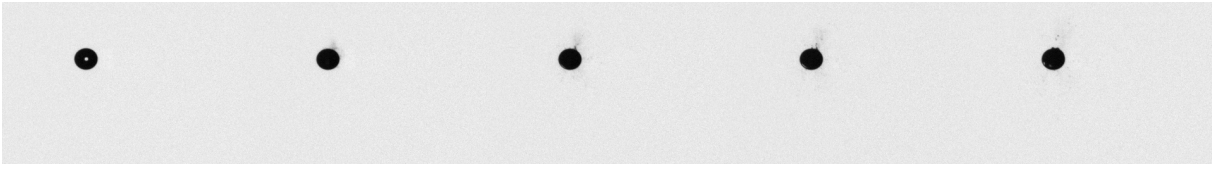

Figure 6: ethanol droplet breakup at 80% laser power.

Decane underwent its first breakup much earlier, at $t = 1.86$ ms. The breakup initiated with subtle ruptures near the rear side of the droplet, resulting in a slight mass ejection. Decane has a higher boiling point (174.1°C) and is less volatile than ethanol, but its lower viscosity and surface tension contribute to early structural instabilities when irradiated.possible cause for this would be Decane's comparatively moderate IR absorption allows some penetration of thermal energy, leading to localized heating and rupture rather than a full vaporization front. The early onset of breakup suggests that breakup or de-

formation, possibly induced by asymmetric thermal expansion or acoustic perturbations, play a key role in its initial deformation.

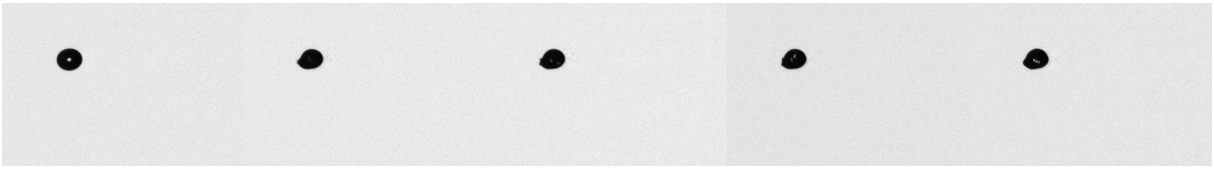

Figure 7: decane droplet breakup at 80% laser power.

Xylene, in contrast, displayed a much more violent and delayed breakup at $t = 16$ ms. The initial response was an abrupt burst, followed by the formation of a bag-like sheet around the droplet, which subsequently disintegrated into smaller fragments. Xylene's higher boiling point (around 138–144°C), and possiblly the stronger IR absorption make it prone to intense energy accumulation. These properties result in significant internal pressure buildup before the breakup. The delayed yet explosive response can thus be attributed to the deep penetration and absorption of laser energy, leading to rapid heating and violent expansion from within the droplet.

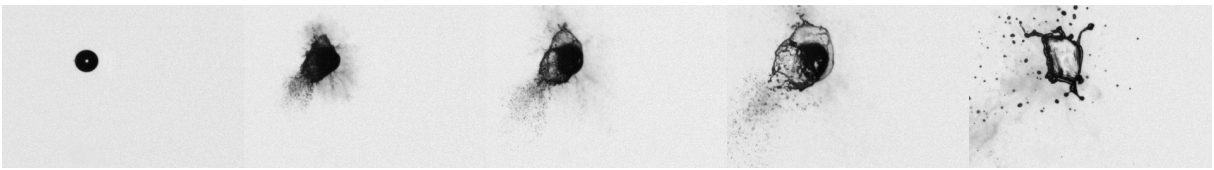

Figure 8: xylene droplet breakup at 80% laser power.

The distinct breakup patterns and timings underscore the role of physical properties in laser-induced droplet breakup phenomena. While ethanol favors vaporization-dominated ejection due to its volatility, decane undergoes rupture , and xylene exhibits explosive disintegration driven by strong absorption and pressure buildup.

4 Conclusion

In this study, laser-induced fragmentation of levitated fuel droplets investigated at different power levels. The image analysis was carried out to understand the nature and timing of first breakup events.

It was observed that the breakup dynamics significantly varied with both the laser power and fluid properties. Xylene exhibited delayed and explosive breakup, ethanol showed a rapid mist-like ejection due to its higher volatility and lower absorption, while decane showed subtle ruptures initially before larger disintegration. The experiments highlight the influence of viscosity, absorption coefficient, and volatility in controlling droplet response to laser irradiation.

These findings are important for future applications in laser-assisted ignition systems and combustion control strategies. Understanding and harnessing the fragmentation behavior can lead to better control over fuel atomization, faster ignition, and more efficient combustion—crucial for aerospace propulsion and micro-thruster systems.

Further research could focus on precisely quantifying droplet size distribution post-breakup, simulating heat transfer mechanisms during irradiation, and expanding to more complex fuel blends and pulse laser configurations.

References

[1] Y. Yi, S. Lv, E. Hu, G. Yin, Y. Zhang, Z. Huang, and Y. Yan, "Laser ignition on single droplet characteristics of aviation kerosene at different pressures and initial diameters: ignition, combustion and micro-explosion," *Journal of the Energy Institute*, vol. 117, 2024, Art. no. 101799. Available: https://doi.org/10.1016/j.joei.2024.101799

[2] V. S. Jagadale, D. C. K. Rao, D. Deshmukh, D. Hanstorp, and Y. N. Mishra, "Modes of atomization in biofuel droplets induced by a focused laser pulse," *Fuel*, vol. 315, 2022, Art. no. 123190. Available: https://doi.org/10.1016/j.fuel.2022.123190

[3] A. Marzo, A. Barnes, and B. W. Drinkwater, "TinyLev: A multi-emitter single-axis acoustic levitator," *Review of Scientific Instruments*, vol. 88, no. 8, 2017. Available: https://pubs.aip.org/aip/rsi/article/88/8/085105/962938/TinyLev-A-multi-emitter-single-axis-acoustic

[4] Tec5USA, *Ultrasonic Levitator Manual*, [Online]. Available: https://www.yumpu.com/en/document/read/10788669/ultrasonic-levitator-manual-tec5usa

[5] NIST Chemistry WebBook, *NIST Standard Reference Database* , Available: https://doi.org/10.18434/T4D303